Supplementary Materials for

Motor skills learning requires new central myelination

Ian McKenzie[1, §], David R Ohayon[1, §], Huiliang Li[1], Joana Paes de Faria[1, 4],

Ben Emery[2], Koujiro Tohyama[3] and William D Richardson[1]

[1] The Wolfson Institute for Biomedical Research, University College London, Gower Street, London WC1E 6BT, UK. [2] Department of Anatomy and Neuroscience and the Florey Institute for Neuroscience and Mental Health, University of Melbourne, Melbourne, Victoria 3010, Australia. [3] The Center for Electron Microscopy and Bio-Imaging Research, Iwate Medical University, 19-1 Uchimuru, Morioka, Iwate 020-8505, Japan. [4] present address: Instituto de Biologia Molecular e Celular, Rua do Campo Alegre 823, 4150-180 Porto, Portugal.
[§] equal contributions, alphabetical order

correspondence to: w.richardson@ucl.ac.uk

This PDF file includes:

> Materials and Methods
> Figs. S1 to S7
> Captions for Movies S1 to S5
> Author contributions

Other Supplementary Materials for this manuscript include the following:

> Movies S1 to S5

Materials and Methods

Mouse breeding and genotyping

$Pdgfra$-$CreER^{T2}$ transgenic mice (2) were crossed with Cre-conditional reporter mice — either $Rosa26R$-YFP ($R26R$-YFP) (11) or Tau-lox-$STOP$-lox-$mGFP$-$IRES$-NLS-$LacZ$-pA (Tau-$mGFP$) (12) — to generate double-homozygous offspring. These were crossed with $Myrf^{(flox/flox)}$ to obtain $Pdgfra$-$CreER^{T2}$: $R26R$-YFP (or Tau-$mGFP$): $Myrf^{(+/flox)}$ offspring, which were sibling-mated to obtain $Myrf^{(flox/flox)}$ and $Myrf^{(+/flox)}$ littermates, which were finally crossed to generate cohorts of $Pdgfra$-$CreER^{T2}$: $R26R$-YFP: $Myrf^{(flox/flox)}$ and $Myrf^{(+/flox)}$ littermates for behavioral analysis.

Genotyping for Cre and $R26R$-YFP was by PCR amplification of genomic DNA as previously described (2). Genotyping for $mGFP$ (encoding a membrane-tethered version of GFP) was with GFP-specific primers (5'-CCCTGAAGTTCATCTG-CACCAC and 5'-TTCTCGTTGGGGTCTTTGCTC). $Myrf^{(flox)}$ mice (9) were genotyped by PCR amplification of genomic DNA using primers within intron 7 flanking the first lox site (5'-AGGAGTGTTGTGGGAA-GTGG and 5'-CCCAGGCTGAAGATGGAATA), which gives a 281 bp product for the wild-type allele and a 489 bp product for the $loxP$-flanked allele.

Our Cre and GFP/YFP reporter lines were maintained separately by crossing (more than 10 generations) with C57B6 females (Charles River; Margate, UK). $Myrf^{(flox/flox)}$ mice were obtained originally (in 2010) on a mixed 129/CBA/C57B6 background. After crossing into a double-homozygous $Pdgfra$-$CreER^{T2}$: $Rosa$-YFP background (predominantly C57B6; 3 generations) they have been maintained by sibling crosses for more than 6 generations and now generate exclusively agouti offspring. They are therefore mixed C57B6/CBA/129 with the major contribution being C57B6 (though agouti coat-color is CBA-derived).

Post-tamoxifen genotyping by reverse transcriptase-PCR

Frontal cortices were dissected from P-$Myrf^{(+/-)}$ and P-$Myrf^{(-/-)}$ mice, one month after tamoxifen administration on P60-P64. Total RNA was prepared using Trizol reagent (Life Technologies) and cDNA generated using the Superscript III kit (Life Technologies). Semi-quantitative PCR was performed using primers corresponding to sequences in exons 7 and 12, either side of the $loxP$-flanked exon 8 (5'-GCCTCAGTGGCTCCTATTTG and 5'-GATCGGAAGGGTGCATAAGA). This gave PCR products consistent with the predicted sizes of 753 bp (unrecombined), 558 bp (exon 8 deleted) and 382 bp (exons 8 and 9 deleted) (8,9) (**Fig. S1**). The latter two bands were excised from the gel, PCR-amplified and sequenced, confirming that the upper band lacked exon 8 and the lower band lacked exons 8 and 9 (not shown). We presume that the presence of a $loxP$ site in the hybrid intron 7/8 formed by Cre-recombination can interfere with normal splicing of the $Myrf$ transcript, resulting in exon 9 skipping. We also presume that the recombined $Myrf$ alleles are transcribed in differentiating OPs that fail to complete OL differentiation and ultimately die because they lack full-length MyRF protein.

Tamoxifen administration

Tamoxifen (Sigma) was dissolved at 40 mg/ml in corn oil by sonicating at 21°C for one hour and administered to postnatal mice by oral gavage on four consecutive days (each dose was 300 mg tamoxifen/Kg body weight). All animal experiments were approved by the UCL Ethical Committee and authorized by the Home Office of HM Government, under the Animals (Scientific Procedures) Act, 1986.

Histochemistry and cell counts

Mice were perfusion-fixed with 4% (w/v) paraformaldehyde (PFA; Sigma) in phosphate-buffered saline (PBS). Brain tissue was dissected and post- fixed in 4% PFA overnight at 4°C. Tissue was cryoprotected in 20% (w/v) sucrose (Sigma) in PBS before freezing in OCT on the surface of dry ice. Coronal cryosections (25 μm) of the brain were collected and processed as floating sections (3). Primary and secondary antibodies were diluted in PBS blocking solution (0.1% [v/v] Triton X-100 and 10% fetal calf serum in PBS) and applied to sections overnight at 4°C. Primary antibodies were anti-PDGFRa (rabbit, New England Biolabs, 1:500 dilution), anti-GFP (chicken, Avas, 1:500) and anti-APC (clone CC1; mouse, Calbiochem,1:200).

Confocal images were collected using an UltraView confocal microscope (Perkin Elmer) with Volocity Software (Perkin Elmer) as Z-stacks with 1 μm spacing, using standard excitation and emission filters for DAPI, FITC (Alexa Fluor-488), TRITC (Alexa Fluor-568) and/or Far Red (Alexa Fluor-647). Cells were counted in low-magnification photo-micrographs (x20 objective) of non-overlapping fields of coronal sections of the corpus callosum, between the dorsolateral corners of the lateral ventricles (6 fields per section, three sections from three or more mice of each genotype).

For Eriochrome cyanine (Eri-C) histochemistry, cryosections on glass slides were rinsed with PBS, immersed in acetone for 5 minutes, rinsed in PBS and submerged in Eri-C solution (Sigma) for 30 minutes. The sections were then differentiated in 5% (w/v) iron alum for 1-10 minutes, followed by a second differentiation step with borax-ferricyanide solution. Slides were then dehydrated and coverslipped. All operations were at ~20°C.

EdU labeling in vivo

To estimate the overall reduction in adult OL genesis stemming from loss of Myrf, we treated P60 *P-Myrf*$^{(+/-)}$ and *P-Myrf*$^{(-/-)}$ littermates with tamoxifen for four days, then administered 5-ethynyl-2'-deoxyuridine (EdU) in the drinking water (0.2 mg/ml) (3) for one week. The animals were analyzed one month later by immunolabeling floating cryosections with monoclonal CC1 and anti-Pdgfra followed by histochemistry for EdU using the AlexaFluor-555 Click-iT detection kit (Invitrogen).

To estimate rates of cell generation in wild type mice during running, EdU was administered as above for the duration of the experiment (up to 3 weeks).

Generation of *Sox10-CreER^{T2}* PAC transgenic mice

To generate *Sox10-iCreER^{T2}* PAC transgenic mice, which express iCreER^{T2} in all oligodendrocyte lineage cells, we modified a mouse phage artificial chromosome (PAC) clone (RP21-427F18, UK Human Genome Mapping Project Resource Centre; **Fig. S3**) that contains 127 kb of genomic DNA spanning the *Sox10* gene locus. The targeting construct was designed to replace the *Sox10* open reading frame with a cassette encoding a tamoxifen-inducible form of codon-improved Cre recombinase (iCreER^{T2}) (*35,36*). The 5′ and 3′ homology regions were first amplified by PCR using the PAC clone as template, then sub-cloned into the targeting vector. A chloramphenicol resistance (*Cm^R*) cassette flanked by *frt* sites was inserted between *iCreER^{T2}* and the 3′ homology sequence. PAC targeting and the subsequent removal of *Cm^R* were performed in *E.coli* strain EL250 by standard methods (*2*). The modified PAC, with the *Sox10* open reading frame replaced by *iCreER^{T2}*, was linearized with NotI and the desired 120 kb band purified by pulsed-field gel electrophoresis for pronuclear injection. Genotyping was by PCR with forward primer specific to intron 2 of *Sox10* (SFAR: 5'-TTGCGATGGGAGAGTCTGAC) and reverse primer specific to *iCreER^{T2}* (iCreAS: 5'-AGGTACAGGAGGTAGTCCCTC) producing a 742 bp product. Four independent *Sox10-iCreER^{T2}* founders were obtained and one selected for further use on the basis of specificity and efficiency of recombination of the *Rosa-YFP* reporter. Approximately 65% of Sox10-immunoreactive cells in the cerebral cortex and corpus callosum, and >90% in the spinal cord, were YFP+ one week after tamoxifen administration to *Sox10-iCreER^{T2} : Rosa-YFP* animals (not shown).

Electron microscopy

Mice were perfusion-fixed at UCL with 100 ml 2.5% (v/v) glutaraldehyde and 2.0% (w/v) paraformaldehyde in 0.1 M cacodylate buffer (pH 7.4). The brains were removed into the same fixative, kept overnight at 4°C and transferred into 0.1M cacodylate buffer for shipment to Japan. 0.5 mm-thick coronal slices were cut with a razor blade and 2 mm squares of tissue including the corpus callosum were processed for electron microscopy (EM). After immersion in a 1% (w/v) osmium tetroxide solution for 2 h at 4°C, the specimens were dehydrated through a graded alcohol series and embedded in Epon 812 (TAAB Laboratories, UK). Semi-thin sections were stained with 0.5% (w/v) Toluidine blue in 0.1 M phosphate buffer, pH 7.4, and imaged in the light microscope (Olympus) equipped with auto-digitizer for "virtual slides" (NanoZoomer-RS, Hamamatsu Photonics). To analyze the whole area of the specimen by EM, ultrathin sections were cut on an ultramicrotome (Ultracut UCT, Leica), collected on a tin-coated glass slide, stained with uranyl acetate and lead citrate and imaged in a scanning EM equipped with a back-scattered electron beam detector (Hitachi SU8010) at 1.0 KV or 1.5 KV accelerating voltage. For further high-resolution examination, the required area was trimmed and smaller ultrathin sections were cut for conventional transmission electron microscopy (TEM). These were stained with uranyl acetate and lead citrate and observed in the TEM (Hitachi H-7650).

<u>Motor</u> <u>behavior</u>

Complex running wheel

We purchased wheel cages (Lafayette Neuroscience) that allow computer-controlled recording of wheel rotation as a function of time for more than 20 cages simultaneously. Mice were maintained on a 12-hour artificial light-dark cycle, caged singly with the running wheel and a small amount of nesting material (tissue paper). Frequently they nested adjacent to the running wheel and occasionally this interfered with wheel rotation; if so, these mice were excluded from subsequent analysis. During running experiments, food and water was replenished every 48 hours (during the light/ inactivity cycle) but otherwise the mice were not disturbed. Wheel rotation was recorded automatically by an infra-red detector. Wheel speed was measured once per hour during the light/ sleep period and at one-minute intervals during the dark/ activity period and data were exported to a spreadsheet, which calculated instantaneous and average speeds over each 24 hour period, as well as accumulated distance run by each mouse.

The mice (postnatal day 60, P60) were caged either with a "regular wheel" with evenly spaced rungs (38 rungs in a 12.7 cm-diameter wheel) or a "complex wheel" from which rungs can be removed to introduce unequal gaps (*13,14*). The complex wheel used in this study had 16 rungs removed to create a 19-rung repeat unit (main text, **Fig. 4A**). The mice ran spontaneously, without artificial reward, on both regular and complex wheels for the equivalent of 5 to 7 Km per night. We routinely clipped their whiskers to prevent them from detecting oncoming rungs in real time (since they run in the dark, visual detection is unlikely). There was a trend (statistically insignificant) for *P-Myrf*$^{(+/-)}$ females to out-perform *P-Myrf*$^{(+/-)}$ males on CW, but no difference between *P-Myrf*$^{(-/-)}$ males and females (**Fig. S5**).

High-speed filming was with a hand-held Casio EX-FH100 digital camera, 240 frames/s, in low-light conditions at the beginning of the dark cycle (~6 pm). Movies were edited on a Macintosh computer using iMovie, converted and compressed on-line (www.zamzar.com).

Accelerating rotarod

Mice were trained for three trials on the rotarod (Ugo Basile) at a constant speed (4 rpm), 120 s each trial. Subsequent weekly test runs consisted of three trials uniformly accelerating from 4 rpm to a maximum of 50 rpm, with mice returned to their home cages for at least 15 minutes between trials.

<u>Statistics</u>

Prism 6.0 (GraphPad) was used for statistical analysis. Running wheel data were analyzed by calculating average speed (m/ minute) for individual mice over each dark cycle, then mean ± s.e.m. for the whole experimental group over the same period. To assess the significance of differences between experimental cohorts at a given time point we used two-way ANOVA with Bonferroni's post-hoc tests. To compare distributions of data points (e.g. distances run by individual mice of *P-Myrf*$^{(+/-)}$ versus *P-Myrf*$^{(-/-)}$ cohorts), we used the Kolgomorov-Smirnov non-parametric test

http://www.physics.csbsju.edu/stats/KS-test.n.plot_form.html. Performance on the rotarod (time to fall) was compared using a similar approach. Cell counts are displayed as mean ± s.e.m. [(s.d./$\sqrt{(n-1)}$ for n<10]. Single time points were compared by Student's t-test.

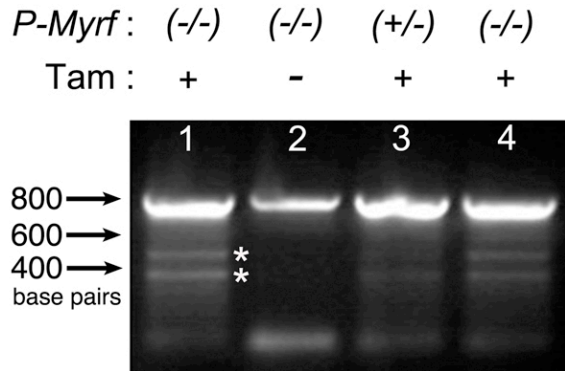**Fig. S1. Cre-mediated recombination in *P-Myrf (flox)* mice.**

Fig. S1. RT-PCR of whole forebrain RNA of tamoxifen (Tam)-treated mice, using exon-7 and exon-12 primers, gave two recombination-specific PCR products above and below 400 bp (*asterisks* in Tam[+] lanes). These lower bands were excised from the low-melting agarose gel, PCR amplified and sequenced, confirming they were derived from *Myrf* transcripts lacking exon 8, or exons 8 + 9.

Fig. S2. Inhibition of OL genesis in adult *P-Myrf* $^{(-/-)}$ mice.

P-Myrf $^{(+/-)}$ *P-Myrf* $^{(-/-)}$

Pdgfra, EdU, CC1
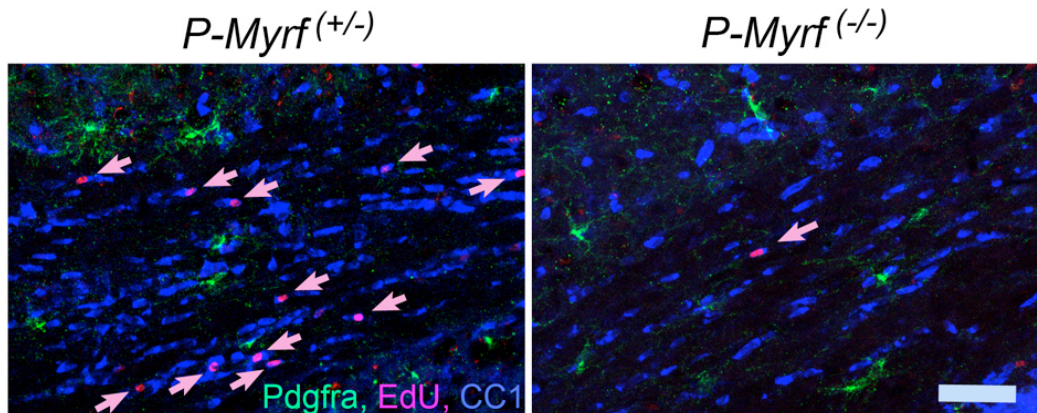
Fig. S2. One month after administering EdU to P60 *P-Myrf* $^{(-/-)}$ mice and their *P-Myrf* $^{+/-)}$ littermates, newly-formed OLs were detected by histochemistry for EdU (red) and CC1 (blue). Many more EdU$^+$, CC1$^+$ cells (arrows) were found in *P-Myrf* $^{+/-)}$ than in *P-Myrf* $^{(-/-)}$ corpus callosum (5.7% ± 0.7% versus 0.20% ± 0.07%; means ± s.e.m., 6 fields (>250 cells) counted in each of 3 sections of 3 mice of each genotype). Therefore, production of new OLs was reduced >95% in the *Myrf* null mice relative to heterozygotes, indicating that the recombination efficiency of *Myrf* $^{(flox/flox)}$ was much greater than the ~57% of OPs that recombined the *Rosa-YFP* reporter (see main text) - presumably because of a more favorable configuration of *loxP* sites. Pdgfra$^+$ OPs (green) are not EdU-labeled in these images because they would have continued to divide during the month following EdU treatment, diluting EdU below the limit of detection. *Scale bar:* 50 μm

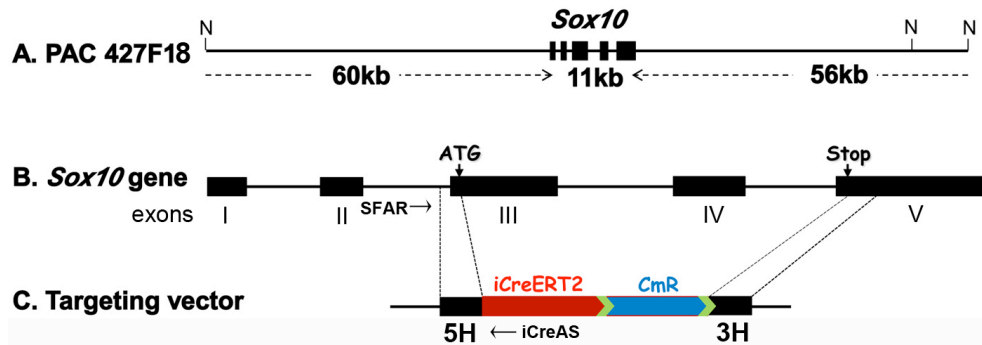**Fig. S3. Generation of *Sox10-iCreERT2 PAC* transgenic mice.**

Fig. S3. (A) PAC clone RP21-427F18 spans the *Sox10* gene with upstream and downstream flanking regions; (B) Diagram of the *Sox10* gene locus; (C) The targeting vector used for homologous recombination. N: NotI site; CmR: chloramphenicol resistance cassette; *green chevrons*: *frt* sites; 5H: 5′ homology region; 3H: 3′ homology region. The positions of genotyping primers (SFAR and iCreAS) are indicated

Fig. S4. Running on CW1 primes mice to run on CW2
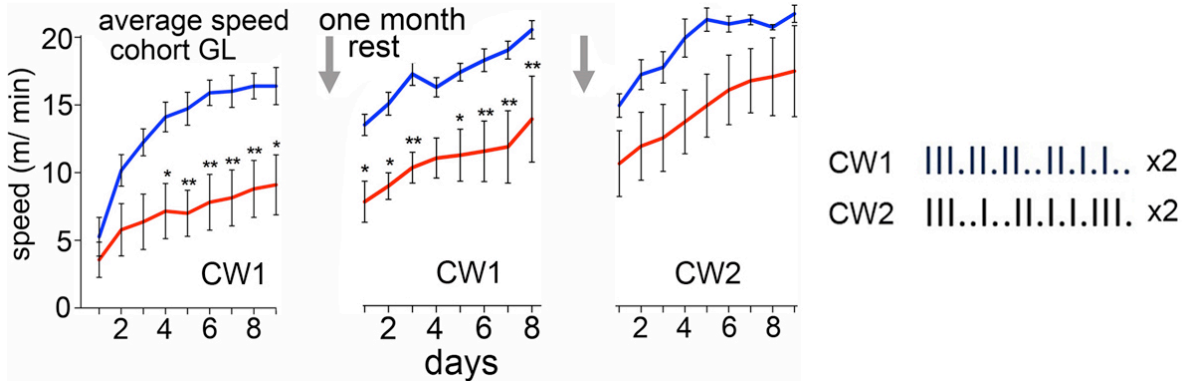
Fig. S4. After tamoxifen, *P-Myrf*$^{(-/-)}$ mice (red graphs) did not learn to run as well on a complex wheel CW1 as their *P-Myrf*$^{(+/-)}$ littermates (blue graphs) (n=6, 7 respectively; also see **Fig. 4E,I** main text). This difference between *Myrf*$^{(+/-)}$ and *Myrf*$^{(-/-)}$ animals persisted when the same cohort was re-tested on CW1 one month later. (*p < 0.05, **p < 0.01). After another week, mice of both genotypes performed at least as well on a second complex wheel with a different rung pattern (CW2) as they did on CW1. Rung patterns are on the right.

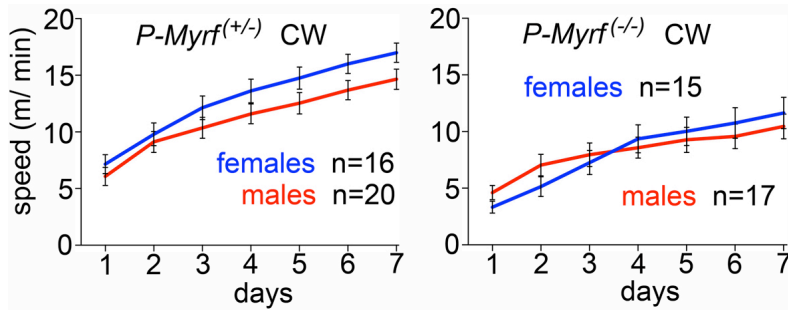**Fig. S5. Complex wheel running abilities of females versus males**

Fig. S5. Female *P-Myrf*^(+/-) mice slightly out-performed their male counterparts on the complex wheel after tamoxifen treatment (experimental design as in **Fig. 4B**, main text), although the difference was not statistically significant (e.g. p=0.52 on day 7; ANOVA with Bonferroni's post-hoc test). (Right) A sex difference was not observed with *P-Myrf*^(-/-) mice.

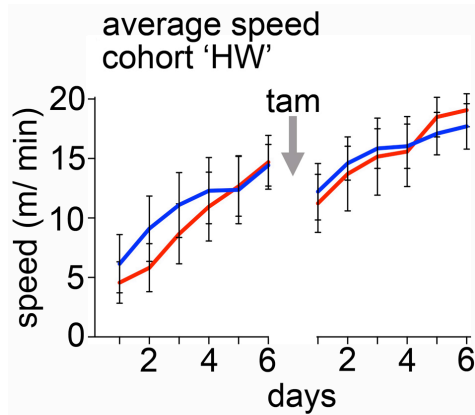**Fig. S6. Adult myelination is not required to perform a pre-learned skill**

Fig. S6. Experimental design was the same as in **Fig. 4M**. *P-Myrf*$^{(+/-)}$ and *P-Myrf*$^{(-/-)}$ mice (blue and red graphs, respectively; n=5 for both groups) were introduced to the complex wheel for nine days before administering tamoxifen. Only six days are shown because data for days 7-9 were lost due to a power failure. Three weeks post-tamoxifen the mice were re-introduced to the complex wheel. Both before and after tamoxifen there was no difference in the performance of *P-Myrf*$^{(+/-)}$ versus *P-Myrf*$^{(-/-)}$.

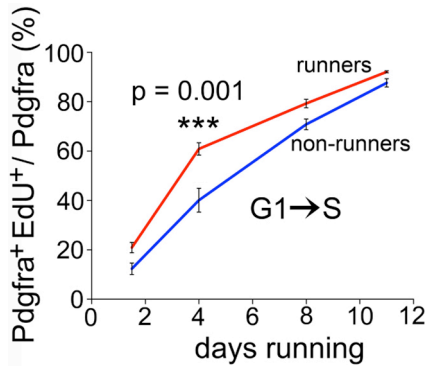**Fig. S7. Running on the regular wheel stimulates OP proliferation**

Fig. S7. Wild type mice were introduced to the regular wheel on P65 and EdU was administered continuously via the drinking water. The EdU labeling index (fraction of Pdgfra$^+$ OPs that was EdU$^+$) was plotted versus time on the wheel. At four days running there was a significant increase in labeling index in runners (red graph) compared to controls without a wheel (blue graph) (p=0.001, n=4; 2-way ANOVA with Bonferroni's post hoc test).

Movie S1. Demyelination-induced tremor in *S10-Myrf$^{(-/-)}$* mice

An *S10-Myrf$^{(-/-)}$* mouse filmed five weeks post-tamoxifen (administered at P60), displaying general ataxia including tremor and momentary seizures typical of advanced de- or dys-myelination.

Movie S2. First introduction to the complex wheel (wt mouse)

A wild type mouse (C57Bl6/CBA F1 hybrid) was filmed during its first introduction to a complex wheel in low light conditions at the beginning of the dark cycle. The movie plays in slow-motion, one-tenth actual speed.

Movie S3. High-speed running on the complex wheel (wt mouse)

A wild-type mouse after seven days' exposure to a complex wheel (low-light conditions at the beginning of the dark cycle). The movie plays at actual speed, interrupted by freeze-frame sequences to show the foot stepping pattern (ipsilateral fore- and hind-paws grasp the same rungs).

Movie S4. *P-Myrf$^{(-/-)}$* mouse on the complex wheel after training

A *P-Myrf$^{(-/-)}$* mouse on the complex wheel after seven nights self-training. A slow-motion sequence (one-quarter actual speed) separates two sequences at actual speed. The mouse appears to run less spontaneously than its *P-Myrf$^{(+/-)}$* littermate (**movie S5**). Although it is difficult to understand the precise problem from movies like this, it seems that placement of the hind paws in particular is less automatic and less accurate.

Movie S5. *P-Myrf$^{(+/-)}$* mouse on the complex wheel after training

A *P-Myrf$^{(+/-)}$* mouse on the complex wheel after seven nights self-training. A slow-motion sequence (one-quarter actual speed) separates two actual-speed sequences.